THE JOURNAL OF PHYSICAL CHEMISTRY B

ARTICLE

pubs.acs.org/JPCB

Effects of Aggregation on the Excitation Dynamics of LH2 from *Thermochromatium tepidum* in Aqueous Phase and in Chromatophores

Fan Yang,[†,‡] Long-Jiang Yu,[§] Peng Wang,[*,†] Xi-Cheng Ai,[†] Zheng-Yu Wang,[§] and Jian-Ping Zhang[*,†]

[†]Department of Chemistry, Renmin University of China, Beijing 100872, People's Repulic of China

[‡]College of Electronic Science and Engineering, Jilin University, Changchun 130012, People's Republic of China

[§]Faculty of Science, Ibaraki University, Mito 310-8512, Japan

Supporting Information

ABSTRACT: We carried out femtosecond magic-angle and polarized pump−probe spectroscopies for the light-harvesting complex 2 (LH2) from *Thermochromatium* (*Tch.*) *tepidum* in aqueous phase and in chromatophores. To examine the effects of LH2 aggregation on the dynamics of excitation energy transfer, dominant monodispersed and aggregated LH2s were prepared by controlling the surfactant concentrations. The aqueous preparations solubilized with different concentrations of *n*-dodecyl-*β*-D-maltoside (DDM) show similar visible-to-near-infrared absorption spectra, but distinctively different aggregation states, as revealed by using dynamic light scattering. The B800 → B850 intra-LH2 energy transfer time was determined to be 1.3 ps for isolated LH2, which, upon aggregation in aqueous phase or clustering in chromatophores, shortened to 1.1 or 0.9 ps, respectively. The light-harvesting complex 1 (LH1) of this thermophilic purple sulfur bacterium contains bacteriochlorophyll *a* absorbing at 915 nm (B915), and the LH2(B850) → LH1(B915) intercomplex transfer time in chromatophores was found to be 6.6 ps. For chromatophores, a depolarization time of 21 ps was derived from the anisotropy kinetics of B850*, which is attributed to the migration of B850* excitation before being trapped by LH1. In addition, the B850* annihilation is accelerated upon LH2 aggregation in aqueous phase, but it is much less severe upon LH2 clustering in the intracytoplasmic membrane. These results are helpful in understanding the light-harvesting function of a bacterial photosynthetic membrane incorporating different types of antenna complexes.

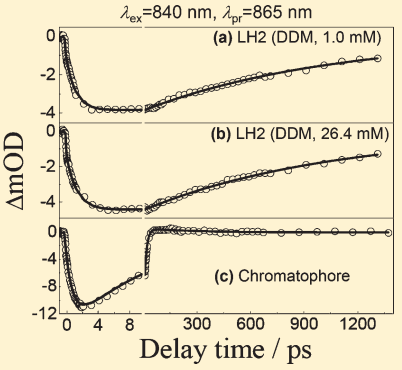

1. INTRODUCTION

In the photosynthetic unit (PSU) of purple bacteria, a core antenna complex (light-harvesting complex 1, LH1) encircling a photosynthetic reaction center (RC) is surrounded by numerous peripheral antennae (light-harvesting complex 2, LH2).[1−3] A major breakthrough in understanding the structure−function relationship of the pigment−protein complexes constituting a PSU is the discovery of the crystallographic structures at atomic resolution, for example, the structures of RCs with spatial resolutions of ∼2 Å for *Blastochloris* (*Bl.*) *viridis*,[4] *Rhodobacter* (*Rb.*) *sphaeroides*,[5] and *Thermochromatium* (*Tch.*) *tepidum*;[6] those of LH2s with 2.0−2.5 Å for *Rhodopseudomonas* (*Rps.*) *acidophila* 10050[7,8] and *Rhodospirillum* (*Rs.*) *molischianum*;[9] and the structure of LH1-RC with a moderate resolution of 4.8 Å for *Rps. palustris*.[10] Recently, the nanoscale spatial organization of LH1-RC and LH2 complexes in an intracytoplasmic membrane (ICM) has been resolved by the use of atomic force microscopy (AFM) and cryo-electron microscopy (cryo-EM).[11,12] On the basis of the aforementioned structural data, a three-dimensional model of the entire membrane vesicle was constructed.[13] The AFM topographs of ICM from various bacterial species reveal that the organization of LH2s with respect to a LH1-RC is diverse. That is, the number of LH2s associated with an LH1-RC is variable (up to seven); there exist clustered LH2 domains lacking of LH1-RC and closely packed LH1-RCs without intermediate LH2s.

The LH2s of *Rps. acidophila* and *Rs. molischianum* consist of nine and eight repeating *α*,*β*-subunits, respectively. In an LH2 of *Rps. acidophila*, 18 bacteriochlorophyll *a* (BChl) molecules (B850) form a ring aggregate that is responsible for the strong optical absorption at ∼850 nm, referred to as the Q_y band, while the remaining 9 BChl molecules (B800) are essentially monomeric, giving rise to a relatively weaker absorption at ∼800 nm. Within an LH2, the averaged separation between adjacent B850 molecules is ∼9 Å, whereas the closest B800−B800 or B800−B850 molecular distance is about twice as large (1.7−2.1 nm). Recent AFM topographic data show that, in ICM, the inter-LH2 B800−B800 and B850−B850 distances are 1.6−2.2 and 2.6−2.8 nm,

Received: October 11, 2010
Revised: May 9, 2011
Published: June 01, 2011

Table 1. Maximal B800 and B850 Absorption Wavelengths (λ^{m}_{B800}, λ^{m}_{B850}) and B850-to-B800 Absorption Ratio ($A_{850\ nm}/A_{800\ nm}$) for LH2s from *Tch. tepidum* at Different DDM Concentrations (cf. Figure 1)[a]

LH2 preparation	λ^{m}_{B800} (nm)	λ^{m}_{B850} (nm)	A_{850}/A_{800}	τ_{EET} (ps)	τ_{B850} (ns)
DDM (1.0 mM)	795	854	1.42	1.1 ± 0.1	1.1
DDM (26.4 mM)	796	854	1.38	1.3 ± 0.1	1.1

[a] Time constants of B800 → B850 transfer (τ_{EET}) and B850* decay (τ_{B850}) (cf. Figure 3).

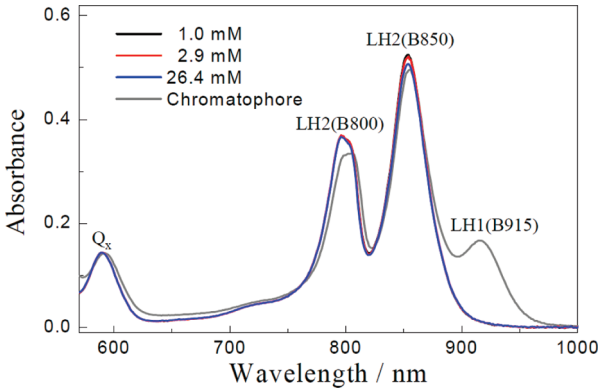

Figure 1. Room-temperature visible-to-near-infrared absorption spectra of solubilized LH2s from *Tch. tepidum* with indicated DDM concentrations. A spectrum of chromatophores is shown for comparison. Spectra are normalized to the Q_x absorption maximum at 590 nm.

respectively,[14] both of which are comparable to the corresponding intra-LH2 separations.

The light-harvesting function of bacterial antennae is based on a series of ultrafast electronic excitation energy transfer (EET) processes. Extensive experimental and theoretical investigations have yielded detailed information for the intra-LH2 and for the LH2−LH1 and LH1−RC intercomplex dynamics (see refs 3 and 15 for recent reviews). For instance, temperature- and excitation-wavelength-dependent intra-LH2 B800 → B850 EET were investigated two decades ago[16−20] or more recently[21−30] for *Rb. sphaeroides* and other bacterial species, and the typical transfer time were determined to be ∼0.7 ps (R.T.) and ∼1.2 ps (77 K); The time scales of intra-LH2 B850 → B850 EET is 50−100 fs, as revealed by time-resolved absorption or fluorescence anisotropy.[31,32] As for intercomplex EET, the LH2 → LH2 transfer time had been found to be in the picosecond (ps) to subnanosecond regime;[27] the LH2 → LH1 transfer time to be reported as several tens of picoseconds at the beginning,[16−18] and further to be refined as 2−5 ps;[3,33,34] and the LH1 → RC transfer time to be 30−70 ps (open RC), respectively.[21,35−38] All the kinetic measurements are performed on chromatophores (membranes)[16−18,20,21,25,27,30,31,33−37,39−43] or isolated complexes[19,22−24,26,32,38] or both of them.[44] On the other hand, the details of both intra- and intercomplex EET processes in a PSU have been theoretically modeled on the basis of the existing cryo-EM, AFM, and crystallographic data, as well as the volumes of kinetics results.[2,45,46] This information, which may be accessible on the basis of the recent advances of structural studies, is important for understanding the EET mechanism of the photosynthetic machinery integrated in ICM.

The photosynthetic bacterium *Tch. tepidum* is a moderate thermophile growing under an optimal temperature range of 48−50 °C.[47] Its pigment−protein complexes exhibit remarkable thermal stability and long-wavelength optical absorption with respect to those of the mesophilic counterparts, such as *Allochromatium* (*Ach.*) *vinosum* and *Rb. sphaeroides*, growing under ∼30 °C.[48] We have recently investigated the LH1-RC complexes from *Tch. tepidum* for the excited-state dynamics, the origin of the high thermal stability, and the mechanism of long-wavelength absorption.[38,49] In the present work, we have examined the population and the depolarization dynamics of isolated and aggregated LH2s in aqueous phase in comparison to those in chromatophores. The results show rather slow intra-LH2 B800 → B850 and intercomplex LH2(B850) → LH1(B915) EET processes and allow the kinetics information concerned with the LH2−LH2 and LH1−LH1 intercomplex EET processes to be derived, all of which are helpful in understanding the roles of antenna clustering in bacterial photosynthetic membranes.

2. MATERIALS AND METHODS

Sample Preparation. Detailed procedures for sample preparation will be presented elsewhere.[50] Briefly, *Tch. tepidum* was cultured anaerobically at 48 °C for 7 days under a light intensity of 2000 lx. The cells were disrupted at 4 °C by ultrasonication, and the chromatophores thus obtained were suspended in 20 mM Tris-HCl buffer (pH 8.5) at a concentration of $OD_{850\ nm}$ = 50 cm^{-1}. After solubilization with 0.35% (v/v) lauryldimethylamine-oxide (LDAO, Kao Corp., Japan) for 60 min in the dark, the suspension was centrifuged for 100 min (145 400*g*, 4 °C). The supernatants as crude LH2s were collected and were further purified with DEAE-cellulose (Whatman DE52) column chromatography in the presence of 0.05% *n*-dodecyl-*β*-D-maltoside (DDM). Visible-to-near-infrared absorption spectra were recorded on a Cary-50 absorption spectrometer (Varian).

Dynamic Light Scattering (DLS). Surfactant and LH2 concentrations are known to be crucial for the aggregation of LH2.[51] We controlled the surfactant concentration to obtain the isolated and aggregated LH2s, and the typical concentrations of DDM (C_{DDM}) used in the present work were 0.05% v/v (1.0 mM) and 1.35% v/v (26.4 mM). Because the critical micelle concentration (CMC) of DDM is 0.1−0.6 mM,[52] the LH2s prepared at the higher and the lower surfactant concentrations are expected to be encapsulated by the surfactant micelles with various sizes in monodispersed or aggregated forms, respectively. The LH2 preparations were filtered with a 0.45 *μ*m ArcoDisk filter immediately before DLS characterization and were thermostatted at 25 °C during the DLS measurements (ALV-5000/E/WIN Multiple Tau Digital Correlator; laser wavelength, 632.8 nm). The scattering light was collected at 90°, and the autocorrelation function was analyzed by using Contin's method.[53] The average hydrodynamic radius, $<R_h>$, was deduced from the diffusion coefficient, *D*, by using the Stokes−Einstein relation, $<R_h> = k_BT/(6\pi\eta D)$.[54]

Time-Resolved Spectroscopy. The apparatus for time-resolved absorption with a 160 fs (fwhm, full width at half-maximum) instrumental response function was previously described in ref 38. Briefly, an optical parametric amplifier (OPA-800 CF-1, Spectra Physics) pumped by a regenerative amplifier

dx.doi.org/10.1021/jp1097537 |J. Phys. Chem. B 2011, 115, 7906–7913

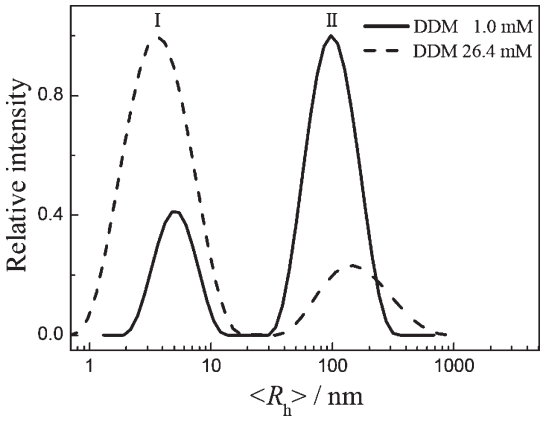

Figure 2. DLS data of the aqueous LH2 preparation of *Tch. tepidum* solubilized with DDM. For C_{DDM} = 1.0 mM, $\langle R_h \rangle_I$ = 5.0 nm and $\langle R_h \rangle_{II}$ = 99.0 nm. For C_{DDM} = 26.4 mM, $\langle R_h \rangle_I$ = 3.6 nm and $\langle R_h \rangle_{II}$ = 155.0 nm.

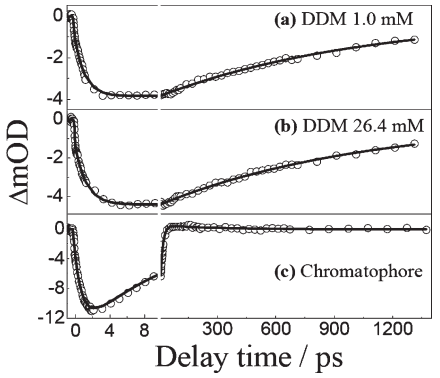

Figure 3. (a, b) Kinetics traces (λ_{ex} = 800 nm, λ_{pr} = 865 nm) for the aqueous suspension of LH2s from *Tch. tepidum* prepared with DDM at indicated concentrations and (c) that for chromatophores. The excitation photon flux density (Φ_{ex}) was 2.0 × 10^{-13} photons·pulse^{-1}·cm^{-2}. Solid curves were obtained by fitting the kinetics to a biexponential model function.

(SPTF-100F-1KHPR, Spectra Physics) provided the actinic laser pulses (~120 fs, fwhm), which was sent to the sample cell (optical path length, 1 mm) with the excitation photon flux density (Φ_{ex}) of 10^{13}−10^{14} photons·pulse^{-1}·cm^{-2}. A white light continuum probe was generated from a 3 mm thick sapphire plate and was detected, after interrogating the excited sample, by the use of a liquid-nitrogen-cooled CCD detector (Spec-10:400B/LN) attached to an imaging spectrograph (SpectraPro 2300i, USA). Time-resolved spectra were corrected against group velocity dispersion. To ensure that each laser shot excites a fresh sample, the laser source was run at the repetition rate of 100 Hz, and the sample cell was kept on shifting across the overlapped actinic and probe beams. The optical density of an LH2 sample at an actinic wavelength was adjusted to 0.2−0.45 mm^{-1}, corresponding to the LH2 concentration of 22−50 μM. Polarized angle pump−probe measurement was used to examine the kinetics of polarization anisotropy, which was obtained by using the relation, $r(t) = (\Delta A_{\parallel}(t) - \Delta A_{\perp}(t))/(\Delta A_{\parallel}(t) + 2\Delta A_{\perp}(t))$, where $\Delta A_{\parallel}(t)$ and $\Delta A_{\perp}(t)$, respectively, refer to the kinetics of paralleling and perpendicular polarization. All of the time-resolved measurements were carried out at room temperature (23 °C). Computer programs for kinetics analysis were compiled based on Matlab (Mathworks) and Mathcad (MathSoft).

3. RESULTS

Characterization of the Aggregation State of LH2s in Aqueous Phase. Figure 1 shows visible-to-near-infrared absorption spectra of the LH2 preparations under different DDM concentrations along with the spectrum of chromatophores. The DDM preparations of LH2s exhibit the Q_y absorption of B800 and B850 at 796 and 854 nm, respectively (Table 1), and the B800 shows inhomogeneous broadening compared to those of LH2s from other bacterial species. The low-temperature absorption of LH2 from the same bacterium gave rise to two distinct B800 Q_y bands with nearly equal amplitudes, suggesting the presence of two forms of B800 with different orientations of Q_y-transition moments.[55] The very recent progress of single protein complexes spectroscopic study[56] excluded the possible contribution of a B850 upper excitonic band in this region.[57,58] The Q_y absorption of B850 is relatively stronger, as is commonly seen for LH2s from other purple bacteria. On increasing the surfactant concentration from 1.0 to 26.4 mM, the Q_y bands vary little in transition wavelengths, and the absorption ratio $A_{850\ nm}/A_{800\ nm}$ drops by only 3%. Compared to the solubilized LH2s, chromatophores exhibit the red-most B800 and B850 absorption peaking at 805 and 855 nm, respectively, as well as an additional near-infrared band at 915 nm originating from the BChls of LH1 (B915). Note that the LH1-Q_y absorption of *Tch. tepidum* is about 40 nm red shifted with respect to the mesophilic purple bacteria, such as *Rb. sphaeroides* and *Rhodosprillum* (*Rs.*) *rubrum*.

Compared to DDM, when LDAO (CMC, 1−2 mM) was used as the surfactant with C_{LDAO} varying from 1.7 to 66.7 mM, a significant blue shift of the B850 absorption (850 → 845 nm) and decrease of $A_{850\ nm}/A_{800\ nm}$ (1.18 → 0.89) were observed (Figure S1, Supporting Information), indicating that LDAO tends to interfere with the LH2 assembly. It is known that solubilized photosynthetic antenna complexes may experience structural deformation and hence spectral variation with respect to their native forms[59] and that the purity and intactness of the LH2s from *Tch. tepidum* depend critically on the nature of the surfactant.[60] For the LH2s from *Rb. sphaeroides*, however, varying the LDAO concentration over a wide range does not cause significant change of the Q_y absorption.[61] Our results imply that, compared to the zwitterionic LDAO, the nonionic DDM with a hydrophilic maltoside moiety favors the intactness of the LH2s from *Tch. tepidum*.

To examine the aggregation behavior of the LH2s, we employed the DLS technique for qualitative characterization, and the representative results are shown in Figure 2. Under C_{DDM} = 1.0 mM, the LH2 preparation exhibits a pair of scattering bands centered at $\langle R_H \rangle$ = 5.0 nm (weaker) and 99.0 nm (stronger). On increasing C_{DDM} to 26.4 mM, the DLS bands shift to $\langle R_H \rangle$ = 3.6 and 155.0 nm, respectively, and the relative intensities are reversed. For each C_{DDM}, two DLS bands are assigned to two sizes of micelles, that is, a smaller one including monodispersed LH2[44] and a larger one including aggregated LH2s. The variation of $\langle R_H \rangle$ under various C_{DDM} is explained by the various size distributions of micelles, because each band includes various amounts of empty micelles, that is, without LH2 incorporated, as shown by the DLS results of an aqueous suspension of DDM alone at a similar concentration (Figure S2, Supporting Information). Taking together the electronic absorption and the DLS evidence, we conclude that DDM is

dx.doi.org/10.1021/jp1097537 |*J. Phys. Chem. B* 2011, 115, 7906–7913

advantageous for the intactness of the LH2 from *Tch. tepidum* irrespective of its dispersive state, while a lower C_{DDM} prefers larger micelles incorporating aggregated LH2s and a higher C_{DDM} prefers smaller micelles incorporating monodispersed LH2 in this study. We could not derive the exact fractions of monodispersed and aggregated LH2s from the DLS data because of the complication from the aggregated empty micelles with unknown shapes and partial specific volumes.[62]

B800 → B850 Excitation Transfer Dynamics. We now examine the dynamics of B800 → B850 EET for isolated or aggregated LH2 preparations. Figure 3 shows the recovery of B850 ground-state bleaching following the pulsed optical excitation at 800 nm. In Figure 3a,b, a rise phase in the initial 8 ps is seen, which is followed by a nanosecond decaying phase. The fast rise is due to the process of B800 → B850 transfer, whereas the slow decay is ascribed to the relaxation of B850 singlet excitation (B850*) living typically for ~1 ns.[63,64] These kinetics could be well accounted for by a biexponential model function comprising a rise and a decay component, and the time constants, τ_{EET} and τ_{B850}, are listed in Table 1. Note that the B800 → B850 transfer time becomes shorter for the LH2 preparation at a lower C_{DDM} (τ_{EET} = 1.1 ps), indicating that the B800 → B850 EET is slightly speeded up upon LH2 aggregation. The B800 → B850 transfer time for LH2s at the high C_{DDM}, τ_{EET} = 1.3 ps, can be regarded as a close approximation to the intrinsic LH2 property, because at such a high C_{DDM} (~40 times of CMC), the aggregation effect is expected to be rather weak. In Figure 3c for chromatophores, both rise and decay phases are considerably accelerated, which are mainly due to the rapid LH2(B850) → LH1(B915) intercomplex EET taking place in a few picoseconds, as well as the effect of weak annihilation among B850* (vide infra).

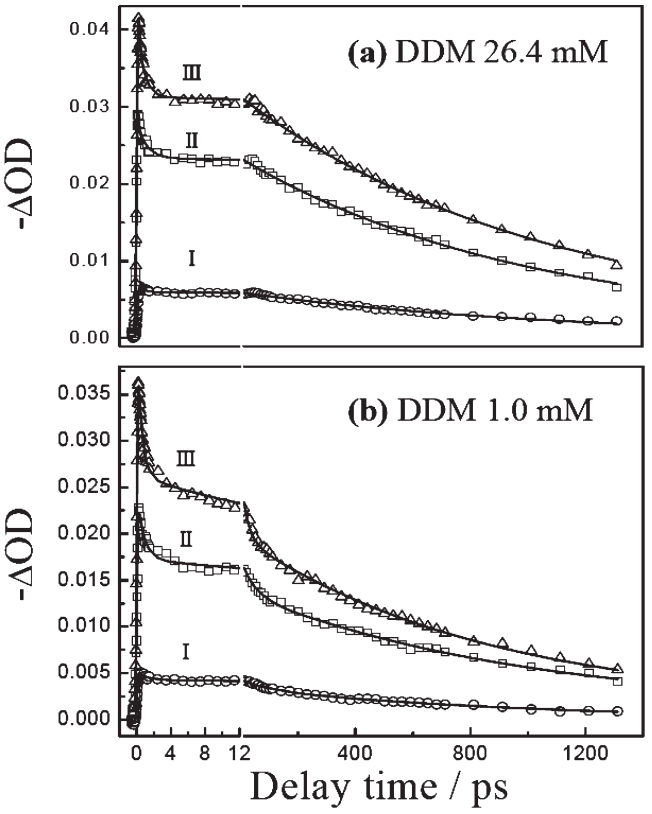

Figure 4. Kinetics traces upon direct B850 excitation of LH2 preparations under indicated DDM concentrations (λ_{ex} = 840 nm, λ_{pr} = 865 nm). Each panel shows the kinetics recorded under three different excitation photon flux densities (Φ_{ex}, photons·pulse^{-1}·cm^{-2}): (I) 2.6 × 10^{13} (○), (II) 1.9 × 10^{14} (□), and (III) 3.7 × 10^{14} (Δ). Solid lines are fitting curves (see text for details).

The B800 → B850 intra-LH2 transfer time is known to be both temperature- and excitation-wavelength-dependent; the values at room temperature are reported to be 0.7 ps for *Rb. sphaeroides*,[19,65] 0.8 ps for *Rps. palustris*,[66] 0.7−0.9 ps for *Rps. acidophila*,[23,24] and 0.7−1.0 ps for *Rs. molischnum*.[24,67] For the LH2 preparation from *Tch. tepidum* with the surfactants (Triton X-100 and sodium dodecyl sulfate) removed completely by column chromatography, the B800 → B850 transfer time was determined to be 0.7−0.9 ps,[23,68] which is in agreement with that determined in the present work for the LDAO preparations (0.9−1.0 ps; Figure S3, Supporting Information). Interestingly, the B800 → B850 transfer time for the isolated LH2s prepared with DDM, 1.3 ps, is considerably slower than those of the chromatophores (0.9 ps) and of the LH2s from the aforementioned bacteria.

Excitation Annihilation in Solubilized LH2 Preparations. When the photosynthetic antennae are exposed to high excitation photon flux, a bimolecular reaction between a pair of singlet excitations (S_1) may take place, $S_1 + S_1 \rightarrow S_1 + S_0$, which is referred to as singlet−singlet annihilation.[69] An important net effect of this reaction is the extinction of an excitation. Figure 4 presents the recovery kinetics of B850 bleaching recorded upon direct photoexcitation of B850. In each panel, the kinetics

Table 2. Decay Time Constants (τ_i, i = 1, 2, 3) with Relative Amplitudes in Parentheses for the 865 nm Kinetics upon Direct B850 Excitation under Different Excitation Photon Flux Densities (Φ_{ex}) for Aqueous LH2 Preparations (cf. Figure 4)

		LH2 preparation	
Φ_{ex} (photons·pulse^{-1}·cm^{-2})	decay component	C_{DDM} = 26.4 mM	C_{DDM} = 1.0 mM
(I) 2.60 × 10^{13}	τ_1 (ps)	0.6 ± 0.4 (19%)	1.5 ± 0.1 (20%)
	τ_2 (ps)		
	τ_3 (ns)	1.1 ± 0.1 (81%)	1.2 ± 0.0 (80%)
(II) 1.90 × 10^{14}	τ_1 (ps)	1.2 ± 0.4 (21%)	0.8 ± 0.0 (31%)
	τ_2 (ps)		36.0 ± 4.0 (15%)
	τ_3 (ns)	1.1 ± 0.1 (79%)	0.9 ± 0.0 (54%)
(III) 3.70 × 10^{14}	τ_1 (ps)	0.5 ± 0.1 (38%)	0.5 ± 0.0 (38%)
	τ_2 (ps)		18.3 ± 1.8 (17%)
	τ_3 (ns)	1.0 ± 0.1 (62%)	0.8 ± 0.0 (45%)

dx.doi.org/10.1021/jp1097537 |*J. Phys. Chem. B* 2011, 115, 7906–7913

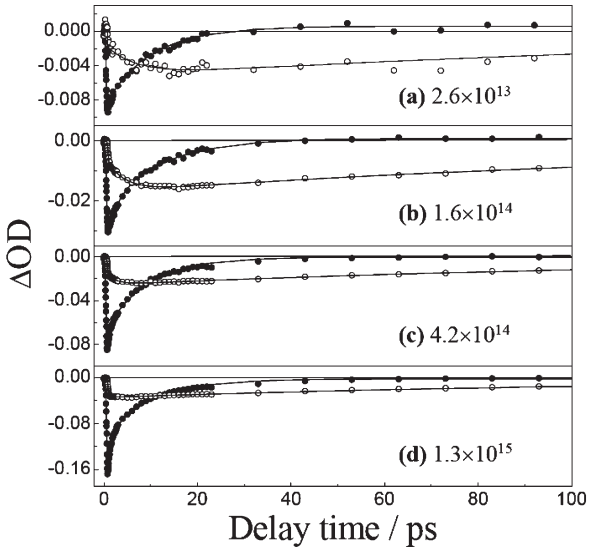

Figure 5. B850 (λ_{pr} = 860 nm, ●) and B915 (λ_{pr} = 920 nm, ○) kinetics traces for chromatophores of *Tch. tepidum* under indicated excitation photon densities (Φ_{ex}, photons·pulse^{-1}·cm^{-2}). The excitation wavelength was 840 nm. Solid lines are fitting curves (see text for details).

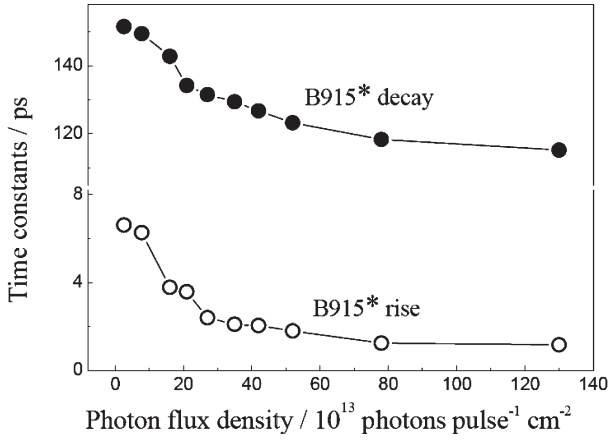

Figure 6. Plots of B915* rise and decay time constants against excitation photon density (Φ_{ex}) for chromatophores from *Tch. tepidum* (cf. Figure 5).

recorded under $\Phi_{ex} \sim 10^{14}$ photons·pulse^{-1}·cm^{-2} (curves II and III) exhibit obvious B850* annihilation, as indicated by the ultrafast decay components with large relative amplitudes in the delay time range of 0−12 ps (see also the kinetics parameters in Table 2), whereas a much less annihilation effect is seen in the kinetics under $\Phi_{ex} \sim 10^{13}$ photons·pulse^{-1}·cm^{-2} (curve I). The major kinetics features are summarized below.

As evidenced by the DLS results, a decrease of DDM concentration from 26.4 to 1.0 mM leads to the transformation of LH2s from monodispersed to aggregated forms. For monodispersed LH2s (Figure 4a), all of the kinetics follow a biexponential decay irrespective of the excitation photon flux density. The shorter decay time constant, $\tau_1 \sim 1$ ps, coincides with the typical time scales of intra-LH2 B850* annihilation, whereas the longer one, $\tau_3 \sim 1$ ns, agrees with the characteristic radiative lifetime of B850* (Table 2). For aggregated LH2s (Figure 4b), the kinetics recorded under $\Phi_{ex} \sim 10^{13}$ and $\sim 10^{14}$, respectively,

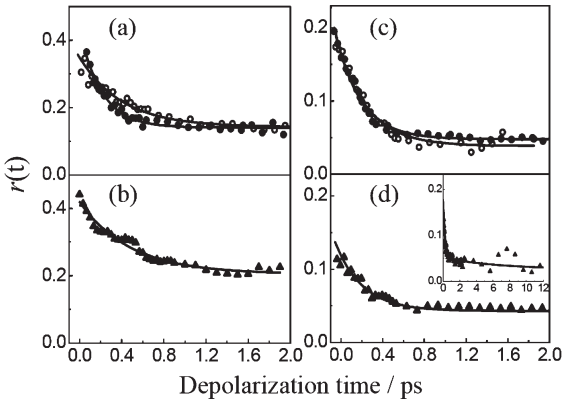

Figure 7. (a) B800* depolarization kinetics for LH2 under C_{DDM} = 26.4 (■) and 1.0 mM (○) and (b) that for chromatophores (λ_{ex} = 800 nm, λ_{pr} = 805 nm). (c) B850* depolarization kinetics for LH2 under C_{DDM} = 26.4 (■) and 1.0 mM (○) and (d) that for chromatophores (λ_{ex} = 840 nm, λ_{pr} = 860 nm). Solid lines are exponential fitting curves without deconvolution to the instrumental response function.

have to be described by bi- or triexponential model functions. The shortest and the longest decay time constants (τ_1 and τ_3) for the three kinetics traces are similar to those of the monodispersed LH2s. However, both kinetics II and III involve an additional decay component with $\tau_2 \approx 36$ and 18 ps, respectively (Table 2). This particular decay phase, which is absent in the kinetics of monodispersed LH2s, must originate from the intercomplex B850* annihilation.

Intra- and Intercomplex Dynamics in Chromatophore. The LH1-Q_y absorption at 915 nm for *Tch. tepidum* is well separated from the LH2-Q_y absorption at 850 nm (Figure 1), which facilitates differentiating the intra- and intercomplex excitation dynamics. We have examined the LH2−LH1 and LH1−LH1 intercomplex excitation dynamics in chromatophores under the direct B850 excitation with Φ_{ex} varied from 2.6×10^{13} to 1.3×10^{15} photons·pulse^{-1}·cm^{-2}. Figure 5 illustrates the representative kinetics of the recovery of B850 and B915 ground-state bleaching.

We first examine the B850 and the B915 kinetics recorded under the lowest Φ_{ex}, which are essentially free from excitation annihilation (Figure 5a). The B850 trace decays monoexponentially with a time constant of 8.7 ps (τ_{obs}). The B915 trace exhibits a rise and a subsequent decays phase: the former is attributed to the intercomplex LH2(B850) → LH1(B915) EET with a the time constant of 6.6 ps (τ_{EET}), which is longer than the values reported for *Rb. sphaeroides* (3.3−4.6 ps),[33,34] whereas the latter decays with a time constant of 150 ps, which is comparable to that of B875* relaxation reported for *Rb. sphaeroides* (140−250 ps).[34,70] Assuming that the decay of the B850 trace is induced by the LH2(B850) → LH1(B915) EET processes together with the B850* radiative decay ($\tau_{B850} \approx 1.1$ ns, Table 2), we would expect a B850* decay time constant of $1/(\tau_{B850}^{-1} + \tau_{EET}^{-1}) = 6.6$ ps. However, this value is considerably shorter than the experimental observation of 8.7 ps, which is to be explained by the excitation migration of B850* before reaching the excitation trap of LH1(B915).

Figure 5b−d shows that a higher Φ_{ex} leads to a more prominent subpicosecond decay in the B850 trace and, concomitantly, a faster rise in the B915 trace, which may be more clearly illustrated in Figure 6. The former is due to the intra-LH2 annihilation of B850*, whereas the latter is presumably due to

Table 3. Depolarization Time Constants (τ_{dep}) of B800* and B850* for LH2s in Aqueous Phase at Different DDM Concentrations and in Chromatophores (cf. Figure 7)

LH2 preparation	λ_{ex} = 800 nm; λ_{pr} = 800 nm τ_{dep} (ps)	λ_{ex} = 840 nm; λ_{pr} = 860 nm τ_{dep} (ps)
DDM (1.0 mM)	0.4 ± 0.0	0.3 ± 0.0
DDM (26.4 mM)	0.2 ± 0.0	0.2 ± 0.0
chromatophores	0.6 ± 0.0	0.2 ± 0.1 (95%); 21.0 ± 7.2 (5%)

the intra-LH1 annihilation of B915* taking place in a typical time scale of <100 fs.[71] In addition, the decay of B915* is also accelerated upon increasing Φ_{ex} (Figure 6), which may be ascribed to the inter-LH1s annihilation of B915* among closely packed LH1s in the ICM.[11,12] Under a similar Φ_{ex}, the B850* annihilation in ICM (Figure 5) is much less severe than that of the LH2 aggregates in aqueous phase (Figure 4b), which may be ascribed to the difference in the aggregation dimensionality of LH2s in aqueous phase (3D) and in ICM (2D) and to the presence of rapid LH2(B850) → LH1(B915) excitation transfer that, in effect, deactivates the B850*.

Depolarization Dynamics of LH2s in Aqueous Phase and in Chromatophores. Figure 7a,b, respectively, presents the anisotropy kinetics of B800* for LH2s in aqueous phase and in chromatophores. Table 3 lists the time constants of depolarization derived from single-exponential curve fitting. For LH2s randomly orientated in aqueous phase, the anisotropic kinetics decay from $r(0)$ = 0.40−0.14 with a C_{DDM}-dependent time constant (0.2−0.4 ps) owing to the intra-LH2 hopping of B800*. Interestingly, the depolarization becomes faster under higher surfactant concentration, indicating the faster randomization of B800* polarization. In the case of chromatophores, the B800* anisotropy drops form $r(0)$ = 0.40−0.20 with a decay time constant of 0.6 ps that is much longer than those of the aqueous LH2 preparations. Although the anisotropy decay of B800* is known to be excitation-wavelength-dependent, the time constants determined in the present work are, in general, shorter than those reported for *Rps. acidophila*, 0.4−0.8 ps,[72] and considerably shorter than those previously reported for the LH2 from *Tch. tepidum* (1.8−3 ps).[23]

The relationship between the rate of depolarization (τ_{dep}) and incoherent excitation hopping (τ_{hop}) of B800* follows $\tau_{dep} = \tau_{hop}/4(1 - \cos^2 \theta)$, where θ is the angle between the Q_y transition dipole moments of adjacent B800 molecules.[23] Here, caution must be taken that this relation is only applicable to the isolated LH2s lacking of intercomplex excitation hopping. The LH2 preparation under C_{DDM} = 26.4 mM is essentially monodispersed with τ_{dep} = 0.2 ps. Assuming that a LH2 comprises nine α,β-subunits with θ = 40°, the time constant of excitation hopping turns out to be τ_{hop} = 0.4 ps, in good agreement with those reported for *Rb. sphaeroides* and *Rps. acidophila*.[31]

It is seen from Figure 7c,d that the B850* excitation depolarizes rapidly from $r(0) \approx 0.20-0.04$ with a time constant of τ_{dep} = 0.2−0.3 ps (Table 3), implying that the randomization of B850* polarization in the B850 ring of an LH2s is extremely fast. Previous anisotropic studies with higher time resolution by means of time-resolved absorption or fluorescence up-conversion spectroscopies had revealed τ_{dep} = 50−90 fs for the LH2s of *Rps. acidophila* and *Rb. sphaeroides*.[23,32] Our results show that the solubilized LH2s and the chromatophores exhibit similar B850* depolarization kinetics; however, the latter exhibits an additional exponential decay component with τ_{dep} = 21 ps (Figure 7d, inset), which is ascribable to the propagation of B850* polarization in clustered LH2s. In this relation, a slow decaying component with a time scale of 26 ps was found for the relaxation of B850* in the chromatophores from *Rb. sphaeroides*, which is attributed to the excitation migration among LH2s before reaching LH1.[34]

4. DISCUSSION

We have characterized, by the use of visible-to-near-infrared electronic absorption and DLS spectroscopies, the aqueous LH2 preparations from *Tch. tepidum* and obtained isolated and aggregated LH2s by adjusting the DDM concentration. In both cases, the intactness of LH2s is maintained, and the intra- and intercomplex excitation dynamics of LH2s were investigated comparatively by means of subpicosecond time-resolved absorption spectroscopies at the magic and the polarized angles. The following discussion will be focused on the intercomplex dynamics of aggregated and clustered LH2s, for which the intra-LH2 excitation dynamics is crucial.

Intra-LH2 B800 → B850 EET. It is known that, although the general tendency of the energy-gap-dependent B800 → B850 transfer time can be predicted by Förster's EET mechanism, the predicted transfer times are often a few times slower than the experimental ones.[28,73−75] A recent theory by G. D. Scholes et al., taking into account the effects of electron−phonon coupling and site energy disorder of the B850 ring aggregate on the donor−acceptor spectral overlap,[76] and that by A. Kimura et al. using the generalized master equation[77] seem promising in modeling the process of B800 → B850 energy transfer. Both of the theories take into account, besides other principal factors, the importance of the excitonic nature of the B850 acceptor.

The rate of B800 → B850 EET can be determined from the rise of B850 bleaching kinetics, or from the decay-to-rise correlation between the B800 and the B850 kinetics.[78] For isolated LH2s, the B800 → B850 EET is regarded as an intracomplex process and, to our surprise, the time constant determined for *Tch. tepidum* in the present work, 1.3 ± 0.1 ps, is considerably longer than those reported for other bacterial species at room temperature (0.7−1.0 ps). Because the multimechanisms possibly dominate the B800 → B850 EET,[76,77] it is not clear at the moment why the B800 → B850 EET for *Tch. tepidum* is rather slow. However, because the absorption spectrum of LH2s from *Tch. tepidum* in the near-infrared region is similar to those of other photosynthetic purple bacteria, the integral of spectral overlap between the B800 emission and the B850 absorption can be similar. Furthermore, the spectral heterogeneity of B800 presenting in the LH2s from *Tch. tepidum*,[55] and its multiple α,β-polypeptide compositions revealed by recent gene sequencing investigations[50] may further complicate the EET mechanisms. Hence more detailed temperature and/or excitation-wavelength-dependent time-resolved spectroscopic studies are needed for a better understanding.

LH2−LH2 Intercomplex Processes. The LH2 aggregation or clustering leads to faster B800 → B850 transfer. For example, for LH2s in aqueous phase, the transfer time was shortened from 1.3 to 1.1 ps upon decreasing C_{DDM} from 26.4 to 1.0 mM (Table 1), and LH2s in chromatophores exhibited the fastest transfer time of 0.92 ps. The B800 → B850 transfer time was even shorter for relatively heavier aggregated LH2 prepared with

LDAO (Figure S3, Supporting Information). The accelerated B800 → B850 transfer upon aggregation is most likely due to the involvement of intercomplex B800 → B850 EET, which is estimated to be 6.6 and 3.0 ps for the LH2 aggregates and the chromatophores, respectively. Recent AFM topographic data show that the B800−B850 separation between the nearest-neighbor LH2s is comparable to that of the intracomplex B800−B850 separation.[14,79] Therefore, both the chromatophores and the LH2 aggregates hold the structural basis for the intercomplex EET as an additional deactivation path of B800*.

The anisotropy kinetics in Figure 7a,b clearly show that the rate of B800* depolarization for the aggregated LH2s (τ_{dep} = 0.4 ps) is much slower than that for the isolated LH2s (τ_{dep} = 0.2 ps). The slower randomization of polarization may be due to the intercomplex hopping of B800* in aggregated LH2s, which effectively prolongates the retention of the excitation polarization. In native ICM, the B800−B800 separation between adjacent LH2s ranges from 1.6 to 2.2 nm depending on their rotational orientation,[14] corroborating the slowest B800* depolarization found for the chromatophores (τ_{dep} = 0.6 ps).

The B850* anisotropy kinetics within the first 2 ps are rather similar from solubilized LH2s (Figure 7c) to chromatophores (Figure 7d), suggesting that the depolarization is mainly caused by the ultrafast intracomplex excitation hopping. However, a second exponential decay with τ_{dep} = 21 ps (5% amplitude contribution) is observed only for the chromatophores (Figure 7d, inset), which can be attributed to the migration of B850* among LH2s prior to being trapped by LH1. As the time scale of LH2 (B850) → LH2 (B850) transfer between closely packed LH2s is estimated to be ∼7 ps,[45] the 21 ps depolarization time implies an average free path of B850* intercomplex migration spanning approximately three LH2s.

LH2−LH1 and LH1−LH1 Intercomplex Processes. It had been shown, by comparing the membranes from wild-type *Rb. sphaeroides* and its mutants, that the LH2(B850) → LH1(B875) transfer times are significantly prolonged upon decreasing the B850−B875 spectral overlap.[33] For the chromatophores from *Tch. tepidum*, the present work has determined the LH2(B850) → LH1(B915) transfer time to be 6.6 ps at room temperature. This value is longer than those of other wild-type bacterial species (3.3−4.6 ps), most likely due to the larger B850−B915 energy gap and hence the smaller spectral overlap. Although earlier studies gave longer transfer times concerning this EET process in *Rb. sphaeroides*, as mentioned in the Introduction, the researchers refined these time constants as 3−5 ps later. Nagarajan et al. assigned the 4.6 ps component as hopping of energy to LH1 from an associated LH2 complex, and the ∼26 ps component to migration of excitations in the LH2 pool preceding transfer to LH1.[34] Finally, the B915* decay time constant is shortened monotonically from 152 to 115 ps upon increasing Φ_{ex} (Figures 5 and 6), which can be explained by the LH1−LH1 intercomplex annihilation of B915*, because the intra-LH1 annihilation of B915* is expected to be much more efficient (<100 fs).

In conclusion, we have shown that DDM as a mild surfactant favors the intactness of the LH2 preparations from the thermophilic purple sulfur bacterium *Tch. tepidum*. At room temperature, the aqueous suspension of isolated LH2s exhibits a B800 → B850 intra-LH2 transfer time of 1.3 ± 0.1 ps, which is considerably slower than those found for the mesophilic purple bacteria. Upon LH2 aggregation in aqueous phase or clustering in chromatophores, this EET process is accelerated considerably by the intercomplex LH2(800) → LH2(B850) process that is estimated to be 6.6 ps (aqueous phase) and 3.0 ps (chromatophores). Other important intercomplex EET processes, including LH2(850) → LH1(B915), excitation migration of B850* among LH2s, and that of 915* among LH1s in chromatophores, have also been examined by comparing the excitation dynamics of LH2 aggregates in vivo and in vitro. As aggregation or clustering of LHs is ubiquitous in the ICM of photosynthetic purple bacteria, the understanding of various intercomplex EET processes is mandatory for a complete picture of the excitation dynamics in photosynthetic membranes.

■ ASSOCIATED CONTENT

Supporting Information. Steady-state absorption spectra and kinetics traces of the LDAO preparations of LH2 and DLS data of the aqueous suspension of DDM alone. This material is available free of charge via the Internet at http://pubs.acs.org.

■ AUTHOR INFORMATION

Corresponding Author

*E-mail: wpeng@chem.ruc.edu.cn (P.W.), jpzhang@chem.ruc.edu.cn (J.-P.Z.). Tel: +86-10-62516604. Fax: +86-10-62516444.

■ ACKNOWLEDGMENT

The project was supported by the National Basic Research Program of China (2009CB220008) and the Natural Science Foundation of China (20933010, 20911120087, 20703067). We are grateful for the support from the Fundamental Research Funds for the Central Universities and the Research Funds of Renmin University of China (10XNI007).

■ REFERENCES

(1) Hu, X.; Damjanović, A.; Ritz, T.; Schulten, K. *Proc. Natl. Acad. Sci. U.S.A.* **1998**, *95*, 5935–5941.
(2) Linnanto, J. M.; Korppi-Tommola, J. E. I. *Chem. Phys.* **2009**, *357*, 171–180.
(3) Sundström, V.; Pullerits, T.; van Grondelle, R. *J. Phys. Chem. B* **1999**, *103*, 2327–2346.
(4) Deisenhofer, J.; Epp, O.; Sinning, I.; Michel, H. *J. Mol. Biol.* **1995**, *246*, 429–457.
(5) Ermler, U.; Fritzsch, G.; Buchanan, S. K.; Michel, H. *Structure* **1994**, *2*, 925–936.
(6) Nogi, T.; Fathir, I.; Kobayashi, M.; Nozawa, T.; Miki, K. *Proc. Natl. Acad. Sci. U.S.A.* **2000**, *97*, 13561–13566.
(7) McDermott, G.; Prince, S. M.; Freer, A. A.; Hawthornthwaite-Lawless, A. M.; Papiz, M. Z.; Cogdell, R. J.; Isaacs, N. W. *Nature* **1995**, *374*, 517–521.
(8) Papiz, M. Z.; Prince, S. M.; Howard, T.; Cogdell, R. J.; Isaacs, N. W. *J. Mol. Biol.* **2003**, *326*, 1523–1538.
(9) Koepke, J.; Hu, X.; Muenke, C.; Schulten, K.; Michel, H. *Structure* **1996**, *4*, 581–597.
(10) Roszak, A. W.; Howard, T. D.; Southall, J.; Gardiner, A. T.; Law, C. J.; Isaacs, N. W.; Cogdell, R. J. *Science* **2003**, *302*, 1969–1972.
(11) Bahatyrova, S.; Frese, R. N.; Siebert, C. A.; Olsen, J. D.; van der Werf, K. O.; van Grondelle, R.; Niederman, R. A.; Bullough, P. A.; Otto, C.; Hunter, C. N. *Nature* **2004**, *430*, 1058–1062.
(12) Scheuring, S.; Lévy, D.; Rigaud, J. L. *Biochim. Biophys. Acta* **2005**, *1712*, 109–127.
(13) Sener, M. K.; Olsen, J. D.; Hunter, C. N.; Schulten, K. *Proc. Natl. Acad. Sci. U.S.A.* **2007**, *104*, 15723–15728.
(14) Sturgis, J. N.; Tucker, J. D.; Olsen, J. D.; Hunter, C. N.; Niederman, R. A. *Biochemistry* **2009**, *48*, 3679–3698.
(15) Cogdell, R. J.; Gall, A.; Köhler, J. *Q. Rev. Biophys.* **2006**, *39*, 227–324.

(16) Frieberg, A.; Godik, V. I.; Pullerits, T.; Timpmann, K. *Chem. Phys.* **1988**, 227–235.
(17) Sundström, V.; van Grondelle, R.; Bergström, H.; Åkesson, E.; Gillbro, T. *Biochim. Biophys. Acta* **1986**, *851*, 431–446.
(18) van Grondelle, R.; Bergström, H.; Sundström, V.; Gillbro, T. *Biochim. Biophys. Acta* **1987**, *894*, 313–326.
(19) Shreve, A. P.; Trautman, J. K.; Frank, H. A.; Owens, T. G.; Albrecht, A. C. *Biochim. Biophys. Acta* **1991**, *1058*, 280–288.
(20) Reddy, N. R. S.; Small, G. J.; Seibert, M.; Picorel, R. *Chem. Phys. Lett.* **1991**, *181*, 391–399.
(21) Zhang, F. G.; van Grondelle, R.; Sundström, V. *Biophys. J.* **1992**, *61*, 911–920.
(22) Monshouwer, R.; de Zarate, I. O.; van Mourik, F.; van Grondelle, R. *Chem. Phys. Lett.* **1995**, *246*, 341–346.
(23) Kennis, J. T. M.; Streltsov, A. M.; Vulto, S. I. E.; Aartsma, T. J.; Nozawa, T.; Amesz, J. *J. Phys. Chem. B* **1997**, *101*, 7827–7834.
(24) Salverda, J. M.; van Mourik, F.; van der Zwan, G.; van Grondelle, R. *J. Phys. Chem. B* **2000**, *104*, 11395–11408.
(25) Pullerits, T.; Hess, S.; Herek, J. L.; Sundström, V. *J. Phys. Chem. B* **1997**, *101*, 10560–10567.
(26) Ihalainen, J. A.; Linnanto, J.; Myllyperkiö, P.; van Stokkum, I. H. M.; Ücker, B.; Scheer, H.; Korppi-Tommola, J. E. I. *J. Phys. Chem. B* **2001**, *105*, 9849–9856.
(27) Freiberg, A.; Timpmann, K.; Lin, S.; Woodbury, N. W. *J. Phys. Chem. B* **1998**, *102*, 10974–10982.
(28) Fraser, N. J.; Dominy, P. J.; Ücker, B.; Simonin, I.; Scheer, H.; Cogdell, R. *Biochemistry* **1999**, *38*, 9684–9692.
(29) Theiss, C.; Leupold, D.; Moskalenko, A. A.; Razjivin, A. P.; Eichler, H. J.; Lokstein, H. *Biophys. J.* **2008**, *94*, 4808–4811.
(30) Brust, T.; Draxler, S.; Rauh, A.; Silber, M. V.; Braun, P.; Zinth, W.; Braun, M. *Chem. Phys.* **2009**, *357*, 28–35.
(31) Hess, S.; Åkesson, E.; Cogdell, R. J.; Pullerits, T.; Sundström, V. *Biophys. J.* **1995**, *69*, 2211–2225.
(32) Jimenez, R.; Dikshit, S. N.; Bradforth, S. E.; Fleming, G. R. *J. Phys. Chem.* **1996**, *100*, 6825–6834.
(33) Hess, S.; Chachisvilis, M.; Timpmann, K.; Jones, M. R.; Fowler, G. J. S.; Hunter, C. N.; Sundström, V. *Proc. Natl. Acad. Sci. U.S.A.* **1995**, *92*, 12333–12337.
(34) Nagarajan, V.; Parson, W. W. *Biochemistry* **1997**, *36*, 2300–2306.
(35) Bergström, H.; van Grondelle, R.; Sundström, V. *FEBS Lett.* **1989**, *250*, 503–508.
(36) Kennis, J. T. M.; Aartsma, T. J.; Amesz, J. *Biochim. Biophys. Acta* **1994**, *1188*, 278–286.
(37) Permentier, H. P.; Neerken, S.; Schmidt, K. A.; Overmann, J.; Amesz, J. *Biochim. Biophys. Acta* **2000**, *1460*, 338–345.
(38) Ma, F.; Kimura, Y.; Zhao, X. H.; Wu, Y. S.; Wang, P.; Fu, L. M.; Wang, Z. Y.; Zhang, J. P. *Biophys. J.* **2008**, *95*, 3349–3357.
(39) Timpmann, K.; Freiberg, A.; Godik, V. I. *Chem. Phys. Lett.* **1991**, *182*, 617–622.
(40) Chachisvilis, M.; Kühn, O.; Pullerits, T.; Sundström, V. *J. Phys. Chem. B* **1997**, *101*, 7275–7283.
(41) Freiberg, A.; Jackson, J. A.; Lin, S.; Woodbury, N. W. *J. Phys. Chem. A* **1998**, *102*, 4372–4380.
(42) Polívka, T.; Pullerits, T.; Herek, J. L.; Sundström, V. *J. Phys. Chem. B* **2000**, *104*, 1088–1096.
(43) Timpmann, K.; Zhang, F. G.; Freiberg, A.; Sundström, V. *Biochim. Biophys. Acta* **1993**, *1183*, 185–193.
(44) Timpmann, K.; Woodbury, N. W.; Freiberg, A. *J. Phys. Chem. B* **2000**, *104*, 9769–9771.
(45) Hu, X.; Ritz, T.; Damjanović, A.; Schulten, K. *J. Phys. Chem. B* **1997**, *101*, 3854–3871.
(46) Novoderezhkin, V.; Wendling, M.; van Grondelle, R. *J. Phys. Chem. B* **2003**, *107*, 11534–11548.
(47) Madigan, M. T. *Science* **1984**, *225*, 313–315.
(48) Kimura, Y.; Hirano, Y.; Yu, L. J.; Suzuki, H.; Kobayashi, M.; Wang, Z. Y. *J. Biol. Chem.* **2008**, *283*, 13867–13873.
(49) Ma, F.; Kimura, Y.; Yu, L. J.; Wang, P.; Ai, X. C.; Wang, Z. Y.; Zhang, J. P. *FEBS J.* **2009**, *276*, 1739–1749.
(50) Sekine, F.; Horiguchi, K.; Kashino, Y.; Shimizu, Y.; Yu, L. J.; Kobayashi, M.; Wang, Z. Y. Manuscript submitted for publication.
(51) Schubert, A.; Stenstam, A.; Beenken, W. J. D.; Herek, J. L.; Cogdell, R.; Pullerits, T.; Sundström, V. *Biophys. J.* **2004**, *86*, 2363–2373.
(52) Bhairi, S. M. *Surfactant*; Calbiochem Corporation: Darmstadt, Germany, 2001.
(53) Provencher, W. S. *Comput. Phys. Commun.* **1982**, *27*, 229–242.
(54) Wang, C. H.; Woodford, J. N.; Jen, A. K.-Y. *Chem. Phys.* **2000**, *262*, 475–487.
(55) van Dijk, B.; Nozawa, T.; Hoff, A. J. *Spectrochim. Acta, Part A* **1998**, *54*, 1269–1278.
(56) Berlin, Y.; Burin, A.; Friedrich, J.; Köhler, J. *Phys. Life Rev.* **2007**, *4*, 64–89.
(57) Koolhaas, M. H. C.; Frese, R. N.; Fowler, G. J. S.; Bibby, T. S.; Georgakopoulou, S.; van der Zwan, G.; Hunter, C. N.; van Grondelle, R. *Biochemistry* **1998**, *37*, 4693–4698.
(58) Leupold, D.; Stiel, H.; Ehlert, J.; Nowak, F.; Teuchner, K.; Voigt, B.; Bandilla, M.; Ücker, B.; Scheer, H. *Chem. Phys. Lett.* **1999**, *301*, 537–545.
(59) Pflock, T.; Dezi, M.; Venturoli, G.; Cogdell, R. J.; Köhler, J.; Oellerich, S. *Photosynth. Res.* **2008**, *95*, 291–298.
(60) Nozawa, T.; Fukada, T.; Hatano, M.; Madigan, M. T. *Biochim. Biophys. Acta* **1986**, *852*, 191–197.
(61) Kangur, L.; Timpmann, K.; Freiberg, A. *J. Phys. Chem. B* **2008**, *112*, 7948–7955.
(62) González-Gaitano, G.; Rodríguez, P.; Isasi, J. R.; Fuentes, M.; Tardajos, G.; Sánchez, M. *J. Inclusion Phenom. Macrocyclic Chem.* **2002**, *44*, 101–105.
(63) Bergström, H.; Sundström, V.; van Grondelle, R.; Gillbro, T.; Cogdell, R. *Biochim. Biophys. Acta* **1988**, *936*, 90–98.
(64) Monshouwer, R.; Abrahamsson, M.; van Mourik, F.; van Grondelle, R. *J. Phys. Chem. B* **1997**, *101*, 7241–7248.
(65) Hess, S.; Feldchtein, F.; Babin, A.; Nurgaleev, I.; Pullerits, T.; Sergeev, A.; Sundström, V. *Chem. Phys. Lett.* **1993**, *216*, 247–257.
(66) Zhao, X. H.; Liang, J.; Ma, F.; Sun, W. J.; Wang, P.; Fu, L. M.; Ai, X. C.; Zhang, J. P. *Chem. J. Chin. Univ.-Chin.* **2008**, *29*, 149–153.
(67) Wendling, M.; van Mourik, F.; van Stokkum, I. H. M.; Salverda, J. M.; Michel, H.; van Grondelle, R. *Biophys. J.* **2003**, *84*, 440–449.
(68) Kennis, J. T. M.; Streltsov, A. M.; Aartsma, T. J.; Nozawa, T.; Amesz, J. *J. Phys. Chem.* **1996**, *100*, 2438–2442.
(69) van Grondelle, R. *Biochim. Biophys. Acta* **1985**, *811*, 147–195.
(70) Freiberg, A.; Godik, V. I.; Pullerits, T.; Timpman, K. *Biochim. Biophys. Acta* **1989**, *973*, 93–104.
(71) Bradforth, S. E.; Jimenez, R.; van Mourik, F.; van Grondelle, R.; Fleming, G. R. *J. Phys. Chem.* **1995**, *99*, 16179–16191.
(72) Ma, Y. Z.; Cogdell, R. J.; Gillbro, T. *J. Phys. Chem. B* **1997**, *101*, 1087–1095.
(73) Hess, S.; Visscher, K. J.; Pullerits, T.; Sundström, V. *Biochemistry* **1994**, *33*, 8300–8305.
(74) Fowler, G. J. S.; Hess, S.; Pullerits, T.; Sundström, V.; Hunter, C. N. *Biochemistry* **1997**, *36*, 11282–11291.
(75) Herek, J. L.; Fraser, N. J.; Pullerits, T.; Martinsson, P.; Polívka, T.; Scheer, H.; Cogdell, R. J.; Sundström, V. *Biophys. J.* **2000**, *78*, 2590–2596.
(76) Scholes, G. D.; Fleming, G. R. *J. Phys. Chem. B* **2000**, *104*, 1854–1868.
(77) Kimura, A.; Kakitani, T. *J. Phys. Chem. B* **2003**, *107*, 7932–7937.
(78) Yang, F.; Yu, L. J.; Wang, P.; Ai, X. C.; Wang, Z. Y.; Zhang, J. P. *Acta Phys.-Chim. Sin.* **2010**, *26*, 2021–2030.
(79) Scheuring, S.; Boudier, T.; Sturgis, J. N. *J. Struct. Biol.* **2007**, *159*, 268–276.